Accident Analysis and Prevention 221 (2025) 108159

Contents lists available at ScienceDirect

Accident Analysis and Prevention

journal homepage: www.elsevier.com/locate/aap

A model based on cyclist fall experiments which predicts the maximum allowable handlebar disturbance from which a cyclist can recover balance

Marco M. Reijne [a], Frank H. van der Meulen [b], Frans C.T. van der Helm [a], Arend L. Schwab [a,*]

[a] Department of Biomechanical Engineering, Delft University of Technology, Mekelweg 2, 2628 CD, Delft, The Netherlands
[b] Department of Mathematics, Vrije Universiteit Amsterdam, De Boelelaan 1111, 1081 HV, Amsterdam, The Netherlands

ARTICLE INFO

Keywords:
Cycling safety
Ex-ante evaluation
Fall experiments
Cyclist characteristics
Bayesian model

ABSTRACT

Falls are a significant cause of injury among cyclists, highlighting the need for effective fall prevention interventions. However, ex-ante evaluation of such interventions remains challenging for engineers designing safer infrastructure and bicycles, as well as for safety professionals developing training programs. This study proposes the Maximum Allowable Handlebar Disturbance (MAHD) — the largest external handlebar disturbance a cyclist can recover from — as a performance indicator for evaluating fall prevention interventions. While bicycle dynamics and cyclist control models have the potential to determine this indicator and simulate interventions, their application is currently limited by a lack of validation in predicting the MAHD and the narrow range of interventions that can be incorporated into existing cyclist control models. To address these limitations, we conducted controlled experiments with 24 participants of varying ages and skill levels, exposing them to impulse-like handlebar disturbances that resulted in both recoveries and falls. This dataset, which includes recorded cyclist falls, supports future validation of bicycle dynamics and control models in predicting the MAHD. In addition, using Bayesian Model Averaging, we identified key cyclist factors influencing the MAHD, with forward speed and cyclist balancing skill being critical predictors. Incorporating these predictors into cyclist control models can substantially improve their practical application. These insights were then used to develop a Bayesian multilevel logistic regression model to predict the MAHD for different types of cyclists. Our findings improve the potential for bicycle dynamics and control models to proactively evaluate cyclist fall prevention methods, contributing to safer cycling environments.

1. Introduction

Falls are a leading cause of serious cycling injuries, accounting for approximately two-thirds of incidents (Schepers et al., 2015). This underscores the need for effective fall prevention interventions (Beck et al., 2016; Schepers et al., 2017; Utriainen et al., 2023). The fall risk relates to the inherent instability of the bicycle–cyclist system, especially in emergency situations involving non-linear dynamics. Balance recovery in such moments requires skill and becomes impossible beyond certain lean and steering angles. Although the mechanics of bicycle stability have been well studied (Meijaard et al., 2007; Kooijman et al., 2011; Schwab and Meijaard, 2013; Schwab et al., 2012), evaluating fall prevention interventions remains methodologically challenging.

Various approaches have been used to evaluate cycling safety interventions, including statistical analysis of crash records (Elvik, 2001; Hoye, 2018; Hellman and Lindman, 2023; Lubbe et al., 2022), surrogate safety indicators from video recordings (Sayed et al., 2013; van der Horst et al., 2014), field-based and experimental studies involving cyclists (de Waard et al., 2010; Vlakveld et al., 2015; Dubbeldam et al., 2017; Andersson et al., 2023; Kircher and Niska, 2024; Andersérs et al., 2024), crash-testing (Niska and Wenäll, 2019; Niska et al., 2022; Peng et al., 2012; Fahlstedt et al., 2016; Baker et al., 2024), and traffic simulation models (Twaddle et al., 2014; Schmidt et al., 2023). However, these methods have limitations in evaluating fall-specific interventions such as balance training programs (Keppner et al., 2023), balance-assist technologies (Alizadehsaravi and Moore, 2023), sloped kerbs (Janssen et al., 2018), and ridable road shoulders (Westerhuis et al., 2020).

Crash data analyses are limited by underreporting of single-bicycle crashes, most of which are falls (Schepers et al., 2015; Utriainen et al., 2023). Surrogate indicators, such as Time-To-Collision or Post Encroachment Time, typically focus on interactions with other road users, ignoring single bicycle crashes, which account for most serious injuries (Utriainen et al., 2023). Studies involving cyclists often rely on indirect and unvalidated indicators, such as perceived safety or

* Corresponding author.
E-mail address: a.l.schwab@tudelft.nl (A.L. Schwab).

https://doi.org/10.1016/j.aap.2025.108159
Received 22 November 2024; Received in revised form 27 June 2025; Accepted 30 June 2025
Available online 6 August 2025

Fig. 1. Overview of the experimental setup, with: 1-treadmill, 2-bicycle, 3-pull force motor (4), 4-pull rope (4), 5-force sensor (4), 6-Speedgoat real-time controller, 7-intelligent harness, 8-soft padding (8), 9-disc wheel cover (2), 10-foot strap (2), 11-mechanical rotation limiter, 12-rear-brake handle, 13-helmet, 14-protective gloves (2), 15-motion capture camera (12), 16-IMU (4), 17-EMG measurement unit (4), 18-folding fence.

lean angles. Crash tests primarily target injury mitigation rather than fall prevention. Moreover, current traffic simulation models overlook bicycle balance and lateral dynamics, which are essential for simulating falls. Thus, while falls are the dominant crash mechanism, it remains difficult to evaluate fall prevention interventions using existing methods.

To address this gap, we propose a novel, proactive evaluation approach based on the Maximum Allowable Handlebar Disturbance (MAHD), defined as the largest lateral disturbance a cyclist can withstand before losing balance, and using bicycle dynamics and cyclist control models to determine the MAHD.

This disturbance-based approach draws inspiration from gait research, where such methods have proven effective for identifying fall risk and evaluating interventions (Bruijn et al., 2013). A similar concept is applicable to cycling. However, past cycling studies have only considered small disturbances using linearised models (Moore, 2012; Schwab et al., 2013). These studies are insufficient for understanding fall risk from large disturbances. Cyclists may respond differently depending on disturbance magnitude because of differences in individual characteristics such as strength or reaction time — a pattern also observed in gait research (Bruijn et al., 2013).

Bicycle dynamics and control models, grounded in physics and control theory, offer a cost-effective approach to proactively evaluate a wide range of fall prevention interventions. However, two key challenges limit their current use. First, existing models have only been validated for small disturbances, not actual falls, making it unclear if they can predict the MAHD. Second, cyclist control models currently rely on abstract control parameters (Schwab and Meijaard, 2013), restricting their applicability to incorporate interventions targeting cyclist control. Improving the practicality of these models requires identifying key cyclist characteristics that influence MAHD.

The long-term goal of this study is to improve the application of bicycle dynamics and cyclist control models for proactively evaluating fall prevention interventions. As a step towards this, we conducted controlled cyclist experiments involving 24 participants exposed to impulse-like handlebar disturbances, resulting in both recoveries and falls. These are the first such experiments to safely simulate actual cycling falls. Using Bayesian Model Averaging and multilevel logistic regression, we identified key cyclist characteristics predicting fall outcomes and estimated each participant's MAHD.

Table 1
Summary of participant characteristics by age group, including number of participants, gender distribution, mean age, length, and weight with standard deviations (S.D.)

Group	#	Gender	Age (y)	Length (m)	Weight (kg)
Young	12	7 ♂, 5 ♀	28.8 (4.1)	1.82 (0.10)	75.2 (13.4)
Old	12	7 ♂, 5 ♀	65.2 (4.9)	1.78 (0.09)	78.0 (11.6)

2. Methods

This section describes the experimental data and the development of a Bayesian multilevel logistic regression model to predict the Maximum Allowable Handlebar Disturbance (MAHD).

2.1. Experimental data

Controlled cyclist experiments were conducted at Delft University of Technology, with approval from the Human Research Ethics Committee (approval no. 1870). Participants cycled on a treadmill while handlebar disturbances of varying magnitudes were repeatedly applied, resulting in both balance recoveries and falls. The threshold beyond which balance could not be recovered was defined as the MAHD.

2.1.1. Participants

Twenty-four participants were recruited, equally divided into two age groups: 20–35 years and 60+ years. Each group included seven men and five women. Heights and weights were comparable across groups and representative of the Dutch population. All participants were in good health, experienced cyclists, and cycled regularly. Participant characteristics are summarised in Table 1.

2.1.2. Experimental set-up

The experimental setup (Fig. 1) included a treadmill, a standard Dutch city bicycle equipped with sensors, a rope-driven perturbation system to apply handlebar disturbances, twelve motion-capture cameras, four EMG sensors, and an intelligent safety harness. The bicycle's forward speed, steer rate, and lean rate were recorded, and the cyclist's motion and muscle activity were measured.

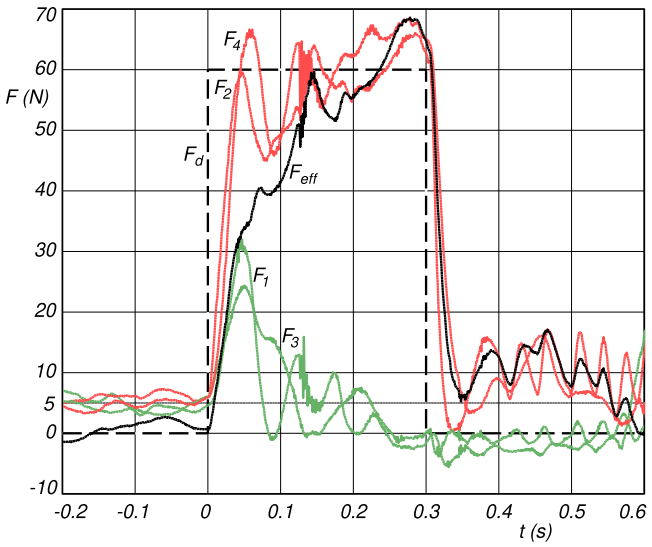

Fig. 2. Disturbance force profile, of the force sensors, for a clockwise handlebar disturbance of 60 N for 0.3 s, with the desired step-like force profile F_d, denoted by the dashed line. This corresponds to an angular impulse ΔL of 18 N ms. The red lines are the measured clockwise forces on the left and right handlebars F_2 and F_4, whereas the green lines are the counterclockwise forces F_1 and F_3. The ropes generating the disturbance forces were positioned relative to the cyclist on the treadmill as follows: rope 1, front right; rope 2, front left; rope 3, rear left; and rope 4, rear right. The black line is the effective force profile $F_{\text{eff}} = (F_2 + F_4 - F_1 - F_3)/2$. All ropes have a controlled pre-tension of 5 N. (For interpretation of the references to colour in this figure legend, the reader is referred to the web version of this article.)

Treadmill and bicycle

Participants cycled on a 2.62 m by 1.2 m treadmill and on a Gazelle Grenoble/Arroyo Elite HMB e-bike (battery removed, small frame size). The participants were allowed to adjust saddle and handlebar positions. All gears were available, and cycling was unassisted.

Disturbances

To determine the MAHD, we applied impulse-like torque disturbances (0.3 s) about the steering axis using a closed-loop, rope-driven perturbation system. Four motor-controlled ropes were attached to the extended handlebars to generate clockwise or counterclockwise torques. Disturbance magnitude was defined in terms of force (easily convertible to angular impulse; see Section 2.1.4). Disturbances were algorithmically selected and manually triggered when the cyclist was riding upright, straight ahead, and centred on the treadmill. An example of a force profile is shown in Fig. 2.

The motors could exert forces up to 200 N with a 44 ms rise time, surpassing typical human reaction latency (Tan et al., 2020). Forces were measured via inline Sciame force sensors. Each motor (260 W Maxon EC-90 Flat, Maxon Group, Switzerland) was controlled by an ECSON 70/10 motor driver. A Speedgoat real-time controller (1 kHz) maintained 5 N pretension during undisturbed cycling and controlled the desired disturbance profile.

The closed-loop force controller used proportional (K_p) and integral (K_i) feedback. Gain tuning resulted in K_p values of 1.5 (motors 1 and 3), 2.00 (motor 2), and 1.75 (motor 4), with a uniform K_i of 2 (1/s). The motors were positioned as follows: motor 1 - front right; motor 2 - front left; motor 3 - rear left; motor 4 - rear right.

Safety precautions

To allow for safe falls, participants wore an intelligent harness (Plooij et al., 2018) suspended from an overhead rail system. It allowed natural cycling movement while providing immediate support during falls (Fig. 3). As a backup, the treadmill was surrounded by angled (45°) padding. During the experiment, the intelligent harness caught the participant every time.

Additional safety measures included a wheel spoke cover and foot straps to prevent entrapment, foam padding on the frame and handlebars, a mechanical stop limiting handlebar rotation to ±45°, relocation of the rear brake lever (centre-mounted) to prevent sudden braking, mandatory use of helmet and gloves, software limits on motor current and a Dyneema carbon-reinforced fishing line (minimal elasticity) tied in series with the ropes to prevent excessive disturbance forces.

These combined precautions ensured that all participants completed the experiment without injury.

2.1.3. Experimental protocol

All participants provided informed consent prior to participation and participated voluntarily. The experimental protocol consisted of two phases: first a familiarisation phase to build trust in the safety harness and learn to cycle on the treadmill, and second the MAHD determination phase.

Familiarisation phase

Participants first practised with the harness, initially standing still and then sitting on the stationary bicycle, to gain confidence that the harness would safely catch them in case of a fall (Fig. 3). They then learned to cycle on the treadmill at a constant speed while gradually releasing a padded support fence, which was folded down once participants were cycling steadily upright and straight ahead. The learning phase was completed when participants could cycle in a controlled manner for several seconds within 10 cm of the left and right borders of the treadmill and for one minute along its centreline. The familiarisation phase typically took 10 to 15 min. Only one participant required longer. Full details of this phase are provided in Supplementary Online Material.

MAHD determination phase

The MAHD was defined as the threshold at which there is a 50% probability the participant will fall. Participants experienced a series of impulse-like handlebar disturbances of varying magnitude and direction while cycling steadily. They were informed prior to the experiment that disturbances would be applied and were instructed to brace themselves and try their best to recover balance.

The outcomes (fall/recovery) were used to fit a logistic regression model. To illustrate this concept, Fig. 4 shows the results of a simple logistic regression analysis applied to example trial data from Fig. 5. In Section 2.2, we describe the more complex Bayesian multilevel logistic regression model used in this study to determine the MAHD for each participant.

An initial MAHD estimate was obtained using a simple staircase procedure. Subsequently, 20 disturbances were applied per speed condition. The disturbance magnitudes were centred around the estimated MAHD and adjusted adaptively using a random adaptive staircase procedure (Doll et al., 2014). This procedure defined a set of five equidistant disturbance forces centred around the moving MAHD estimate, from which each upcoming force was randomly selected. Clockwise and counterclockwise disturbances were applied in random order. Between disturbances, participants repositioned themselves to ride upright, straight ahead, and centred on the treadmill.

Experiments were conducted at 12 km/h initially. Participants could then opt to repeat the protocol at 6 or 18 km/h in randomised order. The familiarisation phase and initial staircase procedure were repeated at each new speed. During the experiments, several participants spontaneously noted that a treadmill speed of 12 km/h felt subjectively comparable to 18 km/h on an open road and a treadmill speed of 18 km/h felt much faster.

Participants could pause or stop the experiment at any time. One participant stopped early, while all others completed at least one set of 20 disturbances at 12 km/h. Minor technical interruptions occurred occasionally and affected trials were repeated as needed. Further details of the staircase algorithm and speed selection rationale are provided in the Supplementary Online Material.

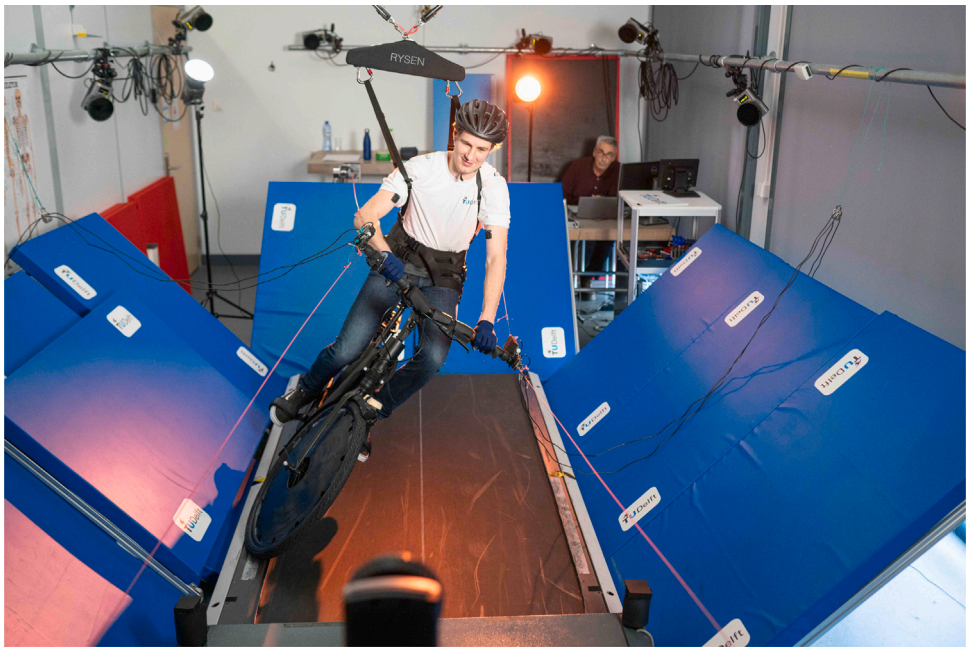

Fig. 3. A snapshot of a situation where the harness caught the participant.

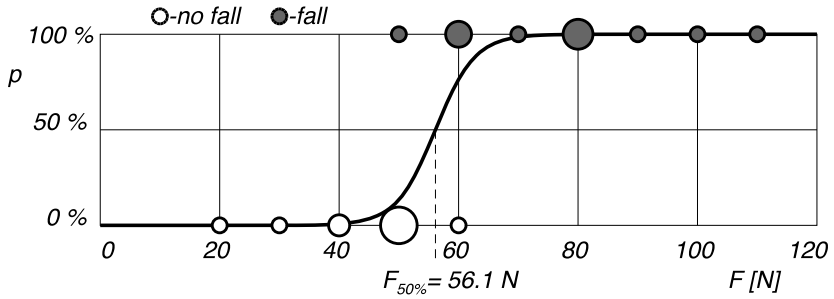

Fig. 4. Example of a logistic regression model applied to the pull force data from Fig. 5. The white dots mark no fall, the dark dots mark a fall, and the area of the dots corresponds to the number of pulls at that specific force value. The solid line is the logistic regression line for the probability p of falling as a function of the pull force F. The pull force for which there is a 50% chance of falling is $F_{50\%} = 56.1$ N. This corresponds to an angular impulse of 13 N ms.

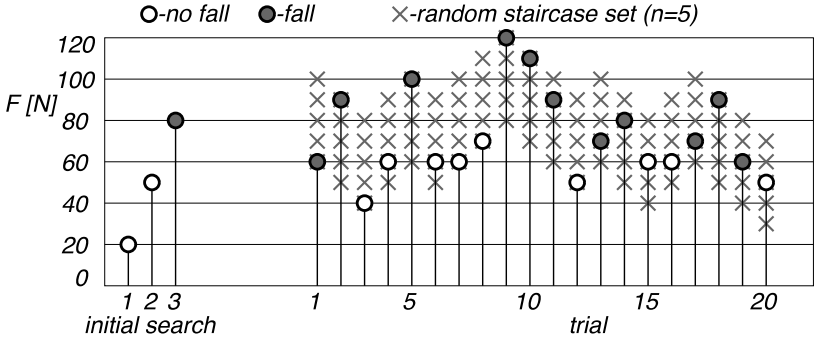

Fig. 5. Example of the random and adaptive staircase procedure to find the MAHD of the pull force F applied at the handlebar for which a cyclist will not fall. White dots mark no fall, dark dots mark a fall, and grey crosses show potential pull forces from which is chosen at random. The initial search is to locate where the random staircase procedure should start.

Table 2
Independent variables collected and considered for the statistical analysis to identify the key variables predictive of fall outcomes and the MAHD.

Symbol	Description	Unit
Trial characteristics		
v	Forward speed	km/h
ϕ_0	Lean angle at the moment the disturbance was applied	rad
$\dot{\phi}_0$	Lean rate at the moment the disturbance was applied	rad/s
δ_0	Steering angle at the moment the disturbance was applied	rad
$\dot{\delta}_0$	Steer rate at the moment the disturbance was applied	rad/s
ψ_0	Heading at the moment the disturbance was applied	rad
$y_{Q,0}$	Lateral position of the ground contact point of the front wheel with Respect to the centre line of the treadmill at the moment the Disturbance was applied	mm
Disturbance characteristics		
ΔL	Angular impulse (magnitude of the applied handlebar disturbance)	N ms
j	Identification number of disturbance	–
d	Rotational direction of the disturbance, where 0 is a counterclockwise Disturbance and 1 a clockwise perturbation	–
y	Outcome of disturbance, where 0 is a recovery of balance and 1 is a fall	–
Task-unrelated participant characteristics		
a	Age	years
m	Mass	kg
h	Length	m
g	Gender, where 0 is female and 1 is male	–
i	Identification number of participant	–
Task-related participant characteristics		
S	Balancing control skill performance	mm
E	Balancing control effort	rad^2/s
τ	Reaction time of participant to applied disturbance	s

2.1.4. Data collection

This study focuses on identifying cyclist control characteristics that predict falls and the MAHD. We collected general — task-unrelated — participant characteristics and task-related characteristics. In addition, we measured bicycle states as well as trial and disturbance parameters. A summary of all variables is provided in Table 2, and details are described below.

Task-unrelated participant characteristics

Age (a), height (h), and gender (g) were self-reported. Mass (m) was measured prior to the experiment with participants wearing the protective gear. Finally, each participant was assigned a unique identifier (i).

Task-related participant characteristics

Balancing control skill (S) and effort (E) were determined from a one-minute undisturbed cycling task at each forward speed. Prior to the application of disturbances at that speed, participants were instructed to maintain balance and follow a marked centreline on the treadmill for one minute.

Balance control skill (S) was defined as the standard deviation of the lateral front wheel position relative to the treadmill centreline (y_{fw}), reconstructed from Qualisys motion capture data (100 Hz) using rigid body constraints and least-squares methods. Balance control effort (E) was computed as the integral of squared steer rate ($\dot{\delta}$), derived from an IMU on the front fender (Delsys Trigno EMG sensor). This data was collected at 2 kHz and smoothed using a second-order low-pass Butterworth filter with a cutoff frequency of 20 Hz.

Reaction time (τ) was determined for each disturbance from EMG signals recorded on both biceps and triceps. The raw data was rectified, normalised, and smoothed using a second-order low-pass Butterworth filter with a cutoff frequency of 40 Hz. Reaction time was defined as the first point at which any of the four EMG signals exceeded twice the standard deviation of the baseline signal during the second before $t = 0$. Here, $t = 0$ was defined as the time after the operator triggered the disturbance and when any of the four pull force measurements exceeded twice the baseline standard deviation of the force signal one second prior.

Trial and disturbance characteristics

Forward speed (v) was set by the treadmill (6, 12, or 18 km/h). Bicycle states at the moment the disturbance was applied — lean angle (ϕ_0), lean rate ($\dot{\phi}_0$), steering angle (δ_0), steer rate ($\dot{\delta}_0$), heading (ψ_0), and lateral position of the front wheel ground contact point ($y_{Q,0}$) — were reconstructed from motion capture data.

The disturbance magnitude (ΔL), defined as the angular impulse, was calculated from the effective force applied by four rope-driven actuators (measured at 1 kHz), multiplied by half of the handlebar width ($w_h = 0.82$ m), disturbance duration ($\Delta t = 0.3$ s), and corrected for steer axis tilt ($\lambda = 21.5°$), by

$$\Delta L = (F_2 + F_4 - F_1 - F_3)\frac{w_h}{2}\cos(\lambda)\Delta t. \quad (1)$$

Each disturbance was labelled with an identifier (j) and rotational direction (d; 0 = counterclockwise, 1 = clockwise). Fall outcome (y) was manually classified per trial ($y = 1$ if the participant fell, $y = 0$ otherwise), based on observable events (e.g., a fall, foot placement or riding off the treadmill).

Synchronisation

EMG and motion capture data were synchronised via Qualisys Track Manager. Disturbance data from the Speedgoat real-time controller was synchronised with the Qualisys Track Manager via an analog signal representing the desired disturbance force.

2.2. Statistical modelling

In analysing the collected experimental data, we start with exploratory data analysis. We adopt the Bayesian approach to statistics to facilitate uncertainty quantification and derive a multilevel logistic regression model. For general background on Bayesian multilevel regression modelling we refer to Gelman et al. (2013). We have centred and scaled all numerical predictors to have average zero and unit standard deviation. We use Bayesian Model Averaging to choose relevant variables. These are chosen to be those variables which are in the posterior median model (Barbieri and Berger, 2004; Clyde et al., 2011). We then refine the model based on the chosen set of variables by

taking into account the multilevel structure of the data. Clearly, such a structure is present in the data because experiments can be grouped by participant.

From the obtained multilevel logistic regression model we derive the posterior distribution of $\Delta L_{50\%}$, which we define as the angular impulse for which a participant has chance 50% of falling (i.e. our definition of the MAHD). In Sections 2.2.1–2.2.3 below, we detail the methods used in the statistical analysis.

The dataset, R scripts, additional explanatory notes, additional analyses supporting our modelling choices and robustness checks are available in the Supplementary Online Material.

2.2.1. Bayesian model averaging

In the logistic regression model, we assume

$$y_{ij} \mid \theta_{ij} \overset{\text{ind}}{\sim} \text{Ber}(\theta_{ij})$$

with $\log(\theta_{ij}/(1-\theta_{ij}))$ being modelled by linear combination of the available predictors. Suppose the coefficient of the kth predictor in the model is α_k. With p predictors, there are 2^p possible models. In the Bayesian approach, we equip each of these models with a prior probability. If additionally a prior on the coefficients $\alpha_1, \ldots, \alpha_p$ is imposed, the posterior probability of each of the models can be derived. In general, the computations can be intensive, and approximation- or sampling methods may be required. For the logistic regression model this topic is covered in Clyde et al. (2011). Bayesian Model Averaging (see for instance Hoeting et al., 1999) encapsulates the idea that there may be multiple models that explain the data and predictions should be aggregated over predictions within all models, weighted by their posterior probabilities. In our setting, however, besides model prediction, we also care about finding those predictors that are relevant, hoping that some predictors are irrelevant (and therefore need not be recorded) for the prediction of the outcome. Barbieri and Berger (2004) advocate the *median probability model* which is the model that only includes all predictors which have posterior inclusion probability exceeding 1/2. It is this approach we follow here, using the R-package `BAS` (Clyde, 2022). Specific settings (including the prior specification) can be found in the online supplementary material. In the search over models, we impose that angular impulse ΔL is always included in the model. Furthermore, we impose that the identification number of the participant i is treated as one factor, which is either in- or excluded from the model.

2.2.2. Multilevel logistic regression model

The dataset comprises multiple observations per participant. By using the grouping variable participant β_i we induce a hierarchical (multi-level) structure as one can expect that some participants simply perform better than others.

The very simplest model that takes the grouping structure into account is the following.

$$\begin{aligned} y_{ij} \mid \theta_i &\overset{\text{ind}}{\sim} \text{Ber}(\theta_i) \\ \Lambda(\theta_i) &= \beta_i \\ \{\beta_i\} &\sim \text{N}(\bar{\beta}, \sigma_\beta^2). \end{aligned} \tag{2}$$

Here $\Lambda(x) = \log(x/(1-x))$ and $\text{Ber}(\theta)$ denote the logit-function and Bernoulli-distribution respectively where θ_i denotes the probability of falling for the ith participant. The bottom line specifies the prior distribution of the model parameters. One disadvantage of this model is the data for each participant are analysed separately. A multilevel model rightfully acknowledges that these participants are part of a larger population and share common features: data of one participant may help predict if a similar participant will fall in a particular setting. This pooling (sharing) of information is a key idea in multilevel models. Within the Bayesian viewpoint taken here, this can be accomplished by providing priors on $\bar{\beta}$ and σ_β^2.

Another apparent disadvantage of the model specified in Eq. (2) is that it *only* takes participant variation into account. Potentially better models can be obtained by adding variables. Let $x_{ij} = \left(x_{ij}^{(1)}, x_{ij}^{(2)}, \ldots, x_{ij}^{(n)}\right)$ denote a vector of n variables. Then we propose the following model

$$\begin{aligned} y_{ij} \mid \theta_{ij} &\overset{\text{ind}}{\sim} \text{Ber}(\theta_{ij}) \\ \Lambda(\theta_{ij}) &= \beta_0 + \beta_i + \sum_{k=1}^{n} \alpha_k x_{ij}^{(k)} + \gamma \Delta L_{ij} \\ \{\beta_i\} &\overset{\text{iid}}{\sim} \text{N}(0, \sigma_\beta^2) \\ \beta_0, \{\alpha_k\}, \gamma &\overset{\text{iid}}{\sim} \text{N}(0, \sigma^2) \\ \sigma_\beta &\sim \text{half-t}_3(2.5). \end{aligned} \tag{3}$$

Recall that for this model it is assumed that all numerical predictors have been centred and scaled and that we imposed that angular impulse ΔL is always included in the model. For the results presented, we took $\sigma = 2$. We comment on sensitivity to this choice in Section 2.2.4. We used the `brms`-library in the R-language (Bürkner, 2017) to get posterior samples for the model specified in Eq. (3). For σ_β we used the default half Student-t prior with 3 degrees of freedom and scale parameter equal to 2.5, which is denoted by half-$t_3(2.5)$.

In addition, to assess the quality of the model, we performed several posterior predictive checks. These checks can be found in the online supplementary material. In addition, for an excellent accessible exposition on this topic, we refer to Chapter 10 in Lambert (2018).

2.2.3. Maximum allowable handlebar disturbance

We define the MAHD as the angular impulse that induces a 50% chance of falling and use the model described in Eq. (3) to determine the MAHD. Note that 50% is an arbitrary value, but other thresholds can be derived in a similar matter.

The MAHD is the value of the angular impulse for which the probability of falling is equal to 50% (that is, 1/2), denoted by $\Delta L_{50\%}$, and is uniquely determined by the relation

$$\beta_0 + \beta_i + \sum_{k=1}^{n} \alpha_k x^{(k)} + \gamma \Delta L_{50\%} = 0$$

from which we derive

$$\Delta L_{50\%}(x^1, \ldots, x^K) = -\frac{\beta_0 + \beta_i + \sum_{k=1}^{n} \alpha_k x^{(k)}}{\gamma}. \tag{4}$$

The posterior distribution of $\Delta L_{50\%}$ is intractable, but can be approximated using Monte Carlo simulation, since the fitted model provided us with samples from the posterior distribution of $(\beta_0, \{\beta_i\}, \{\alpha_k\}, \gamma)$. Hence, the posterior distribution of $\Delta L_{50\%}$ for participant i can be approximated as follows.

1. take a posterior sample $(\beta_i, \beta_0, \{\alpha_k\}, \gamma)$;
2. compute $\Delta L_{50\%}$ according to Eq. (4);
3. repeat steps (1) and (2) a large number of times.

Here, we see that the Bayesian approach easily allows for uncertainty quantification on $\Delta L_{50\%}(x^1, \ldots, x^K)$. Rather than a simple point estimate, we get its posterior distribution.

For a new participant, not part of the experiment, steps (1) and (2) need a slight adjustment. In this case, we do not have any samples from β_i in step (2). Instead, we first sample σ_β from its posterior and subsequently sample from a Normal distribution with this standard deviation. As a consequence, there will be much higher uncertainty on predictions for people who were not among the participants in the experiment.

To evaluate the model's predictions for 'new' participants, we defined six cyclist types that vary in skill level and forward speed (Table 3). These types were selected to span a range of skill performance S levels and forward speeds. Specifically, $S = 40$ and $S = 90$ represent

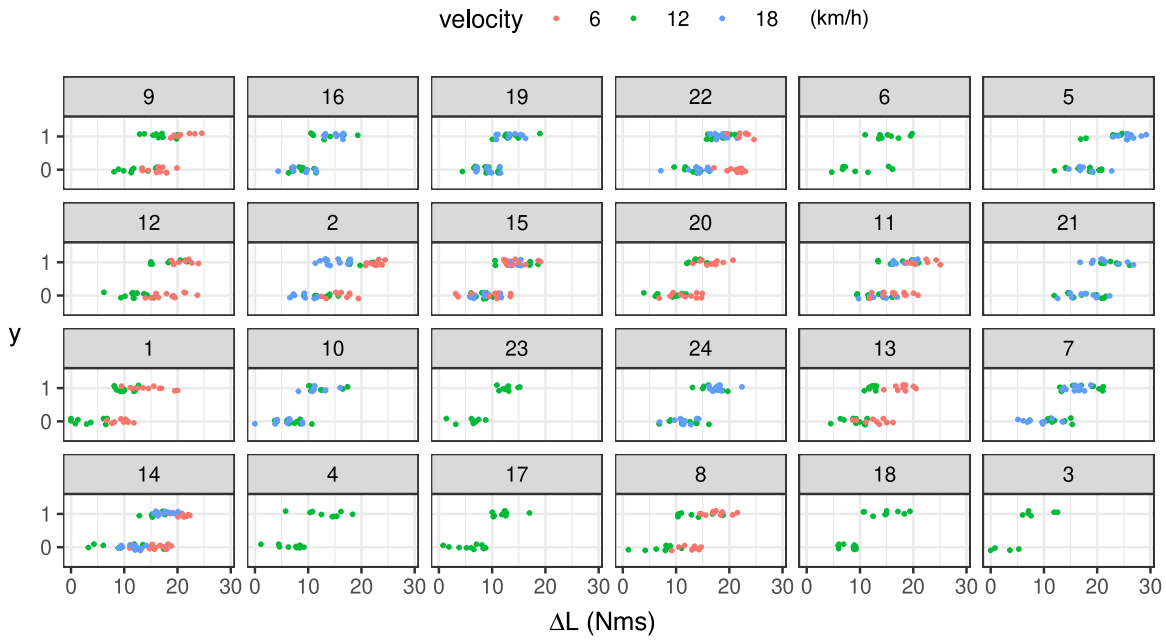

Fig. 6. Each panel corresponds to a participant, ordered by age. The binary outcome variable 'falling' is displayed versus angular impulse. The colouring of points corresponds to forward speed. This figure shows the substantial influence of angular impulse on the outcome variable. (For interpretation of the references to colour in this figure legend, the reader is referred to the web version of this article.)

Table 3
Posterior distribution of parameter $\Delta L_{50\%}$ for six types of cyclists. The name is representative of the characteristics of that cyclist. For example, s40v12 has a skill performance S of 40 mm and cycles at a forward speed v of 12 km/h.

Cyclist type	S (mm)	v (km/h)
s40v12	40	12
s90v12	90	12
s40v6	40	6
s90v6	90	6
s40v18	40	18
s40v25	40	25

the approximate lower and upper bounds observed in the experiments among participants, while the speeds of 6, 12, and 18 km/h reflect the tested speed conditions. One extrapolated case at 25 km/h is included to illustrate the model's prediction slightly outside the experimental conditions. The disturbance number j and disturbance direction were kept constant and were 1 and clockwise, respectively.

2.2.4. Robustness check

To asses robustness of the highest ranked model, we also fitted a generalised linear model including random effects model using the `lme4`-package in R (Bates et al., 2015) and conducted a prior sensitivity analysis by varying σ in the prior to the value 5.

3. Results

A total of 928 observations were collected from 24 participants across one to three forward speeds (Fig. 6). Six participants completed the experiment at 12 km/h only, six at 12 and 6 km/h, six at 12 and 18 km/h, and six at all three speeds. For each set of 20 disturbances per speed, participants experienced at least seven falls and eight recoveries, confirming that the random staircase procedure targeted a 50% fall probability. Only one participant dropped out after 10 disturbances.

Reaction time (τ) was missing for 17 observations due to occasional EMG data loss and approximately 150 observations with implausibly low τ were excluded. Skill performance (S) was missing for one participant at one forward speed (twenty observations) due to marker occlusion. Similarly, four observations of the disturbance direction (d) were missing.

Bayesian Model Averaging results are shown in Figs. 7 and 8. The most probable model (log posterior odds 1.594) included participant ID (i), angular impulse (ΔL), skill performance (S), forward speed (v), disturbance ID (j), disturbance direction (d), lean angle (ϕ_0), and steer rate ($\dot{\delta}_0$). The second-ranked model differed only by excluding d.

Table 4 summarises the posterior distributions for the highest-ranked model. None of the credible intervals from all the variables contains a zero and the Rhat-values indicate no problems with the underlying Hamiltonian-Monte-Carlo method.

Figs. 9 and 10 display the posterior distributions of participant effects (β_i) and independent variable coefficients. The posterior of each β_i seems to be approximately normally distributed and there is more variation in β_i among younger participants than older participants. The posterior distributions of the coefficients of the independent variables also seem to be normally distributed.

Fig. 11 provides a posterior predictive check, indicating reasonable agreement between observed and predicted fall rates across participants and speeds.

Figs. 12 and 13 show posterior distributions of $\Delta L_{50\%}$ (MAHD) for selected participants and hypothetical cyclist profiles, respectively, across different forward speeds.

The results from the robustness check can be found in the online supplementary material. The estimates agree very well with the coefficient estimates obtained within the Bayesian setup. At 5% significance level all included variables are significant. While we have a preference for the Bayesian approach, it is reassuring to see that the frequentist approach gives similar results. We also refitted the Bayesian model in Eq. (3) with σ equal to 5. The results in the latter case are not much different from those presented. If σ is set to 1 we noticed that the estimates get more shrunken towards zero.

4. Discussion

This study provides the first experimental data on cyclist falls and the Maximum Allowable Handlebar Disturbance (MAHD), addressing two key gaps in the application of bicycle dynamics and cyclist control models: the lack of experimental fall data, and the abstract nature of existing cyclist control models. Using controlled fall experiments with 24 participants, we identified key predictors of balance recovery, determined MAHD values, and demonstrated how such models can support proactive evaluation of fall prevention interventions.

Table 4
Results for model defined in Eq. (3) and ranked highest in the heat map (see Fig. 7). The table shows the posterior mean estimate, the estimated error, the lower and upper 95% credible interval, the Rhat values, and the bulk and tail ESS.

Variable	Coeff.	Estimate	Est. error	l-95% CI	u-95% CI	Rhat	$bulk_{ESS}$	$tail_{ESS}$
Intercept	β_0 (–)	0.47	0.73	−0.97	1.90	1.00	8 326	15 883
ϕ_0	α_1 (1/rad)	0.42	0.18	0.08	0.77	1.00	40 802	41 365
d	α_2 (–)	−0.49	0.25	−0.98	−0.01	1.00	46 800	43 224
S	α_3 (1/mm)	0.71	0.22	0.28	1.14	1.00	31 057	39 087
$\dot{\delta}_0$	α_4 (s/rad)	−0.49	0.15	−0.79	−0.18	1.00	45 573	42 651
v	α_5 (h/km)	1.62	0.18	1.27	1.98	1.00	32 852	38 786
j	α_6 (–)	−0.77	0.15	−1.07	−0.48	1.00	43 014	39 719
ΔL	γ (1/N ms)	5.26	0.38	4.55	6.03	1.00	32 380	36 693
sd (Intercept)	σ_β (–)	3.69	0.63	2.66	5.10	1.00	11 420	21 438

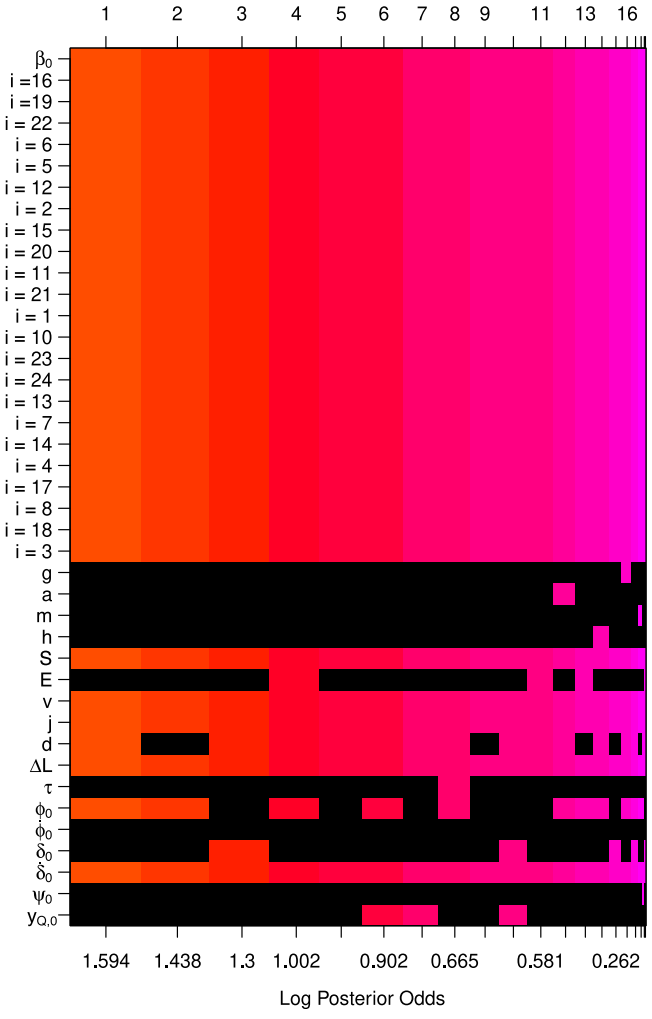

Fig. 7. Heat map of models, ordered along the horizontal axis by their log posterior odds. Black boxes denote that the variable is not in the model. The participant IDs i are ordered according to age.

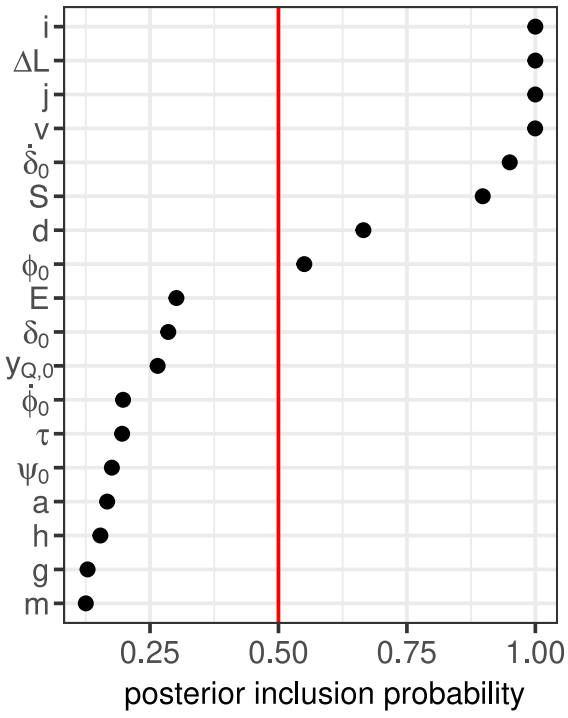

Fig. 8. Posterior inclusion probabilities. Variables which have a probability exceeding 1/2, indicated by the red vertical line, are in the median probability model. (For interpretation of the references to colour in this figure legend, the reader is referred to the web version of this article.)

Disturbance choice

Cycling disturbances that throw a cyclist off balance can arise from impacts (e.g., collisions), uneven surfaces, wind gusts, or unintended steering. While real-world force profiles remain largely unmeasured, impulse-like disturbances offer a reasonable approximation, as many such disturbances occur over short timescales. The chosen 0.3-s constant high torque input provided a sudden disturbance within hardware limits.

Given the coupling of lean and steer dynamics, handlebar disturbances effectively reflect cyclist responses to other impulse-like disturbances beyond a pure handlebar torque disturbance. Moreover, steering into the direction of the fall is the most effective recovery strategy across these types of disturbances (Kooijman et al., 2011). Hence, we believe it is reasonable to assume that if an intervention increases the MAHD, it will also increase the threshold for other disturbances.

While previous studies have applied disturbances to the rear frame via lateral pushes or shifts in tire-ground contact points (Schwab et al., 2013; Bulsink et al., 2016; Dialynas et al., 2023), we chose to apply an impulse-like torque to the handlebars for three reasons. First, the handlebars are highly sensitive, requiring minimal torques to induce falls, thereby improving safety in case of experimental setup malfunctions. Second, rear-frame disturbances demand greater forces than our system can safely generate (Tan et al., 2020). Third, handlebar torques more closely simulate real-world disturbances, while displacing the rear wheel's ground contact point lacks similarity to typical disturbances encountered in real-world cycling.

Cyclist fall experiments

This study was the first to simulate actual cyclist falls. Our experimental setup and protocol proved both practical and safe: only one of 24 participants dropped out, and no injuries occurred — a notably low dropout rate compared to similar fall studies in walking or

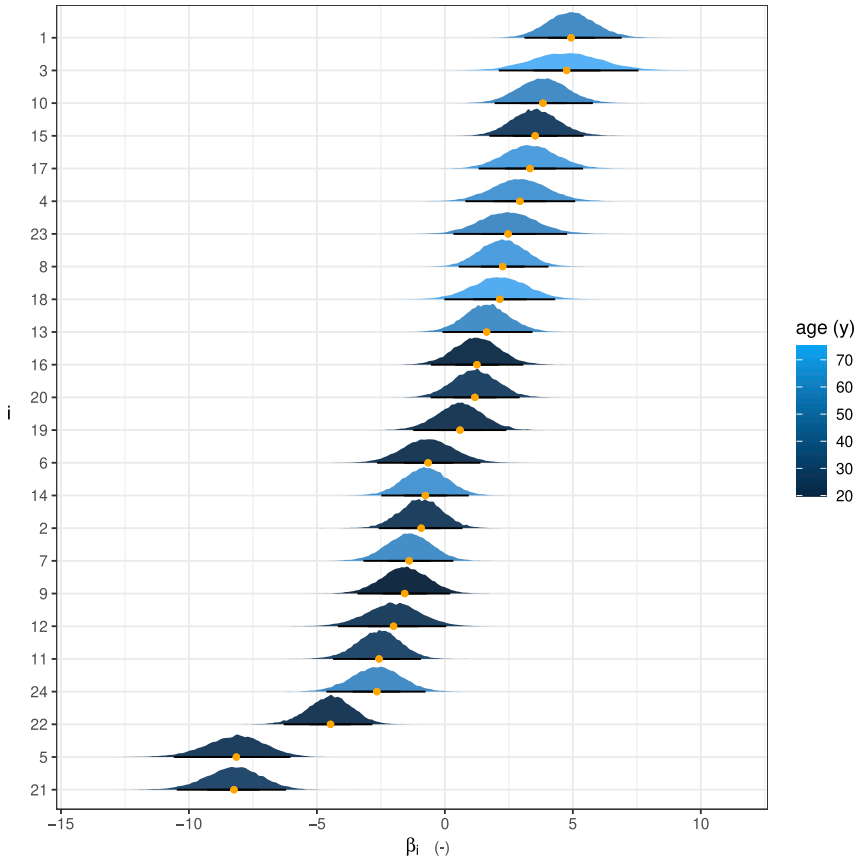

Fig. 9. Posterior distribution of coefficients β_i which represent a baseline for each participant's cycling performance based on the highest ranked model and described by Eq. (3). The coefficients are ordered from the lowest to the highest coefficient. The colour indicates the age of the individual participant. (For interpretation of the references to colour in this figure legend, the reader is referred to the web version of this article.)

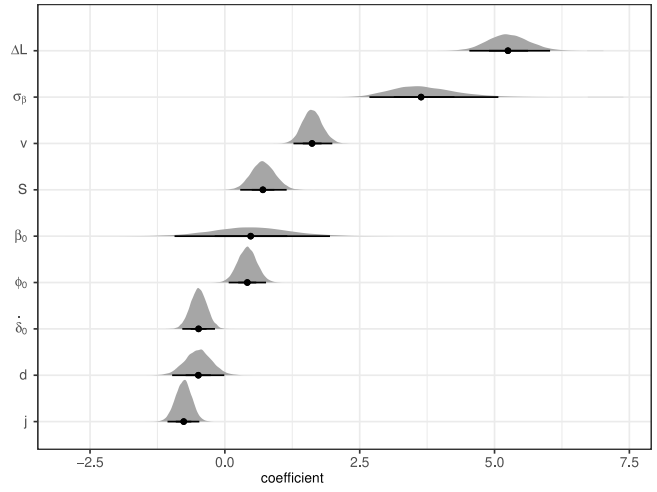

Fig. 10. Posterior distribution of the coefficients, shown in Table 4, for the highest ranked model.

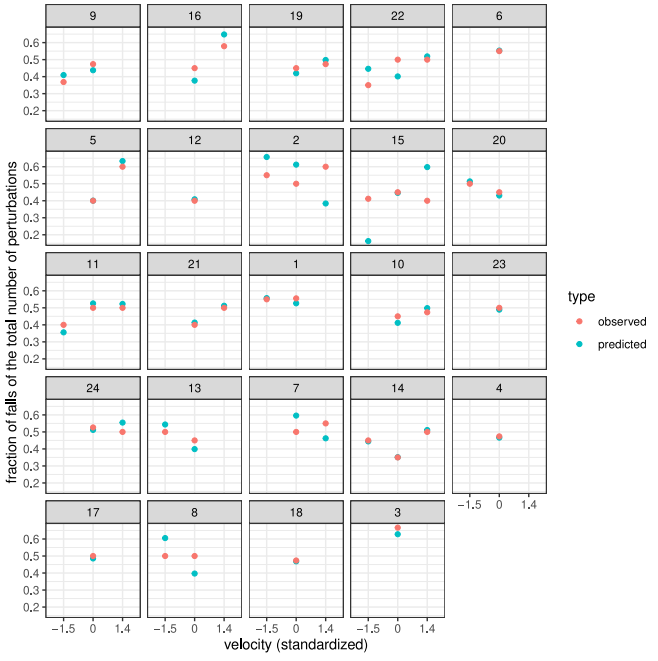

Fig. 11. Posterior predictive check for the highest ranked model: fraction of falling per total number of disturbances for each participant and each forward speed, both observed in the experimental data and as predicted by the highest ranked model.

standing (Pijnappels et al., 2008; Crenshaw et al., 2018). While some participants initially expressed anxiety, this dissipated after their first fall.

A key limitation is the use of a treadmill, which may affect environmental validity. This choice prioritised safety and measurement accuracy. While straight-ahead cycling dynamics at constant forward speed are comparable to real-world cycling, sensory inputs differ. Most participants required several attempts to cycle steadily on the treadmill,

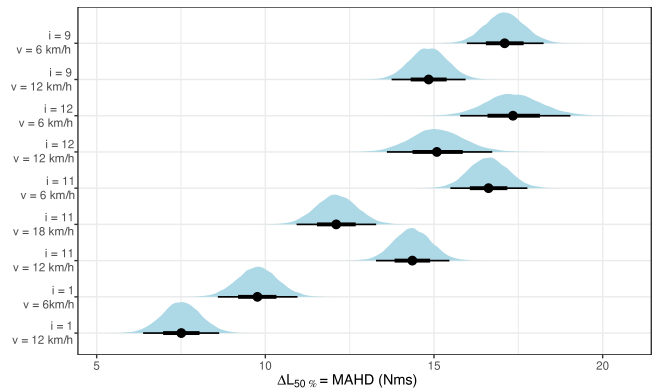

Fig. 12. Posterior distribution of parameter $\Delta L_{50\%}$, which is equivalent to the MAHD, for participants 1, 9, 11 and 12 at different tested forward speeds v (km/h) indicated in the labels on the vertical axis.

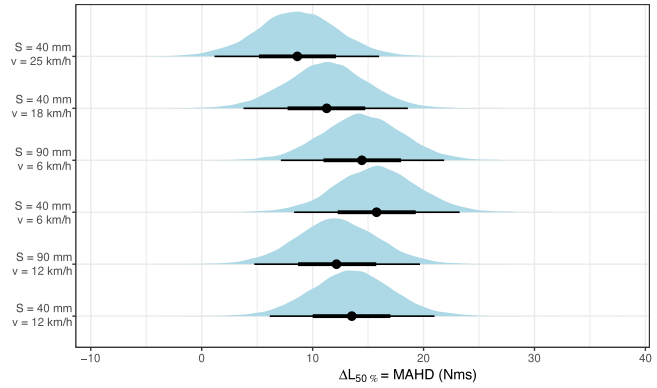

Fig. 13. Posterior distribution of parameter $\Delta L_{50\%}$, which is equivalent to the MAHD, for 6 types of cyclists, with characteristics as displayed in Table 3.

and many perceived 12 km/h on the treadmill as equivalent to higher speeds outdoors. The potential impact of treadmill cycling on cycling behaviour requires further investigation.

Participants were briefed about the upcoming disturbances. Consequently, the MAHD values reported here may be considered optimistic. Randomisation of disturbance direction, magnitude, and timing helped mitigate predictability, yet the sequence number j still influenced MAHD, with later trials showing higher thresholds.

Finally, the experimental dataset can be used for validating bicycle dynamics and cyclist control models for large disturbances close to the fall threshold. The recorded transient responses before, during, and after disturbances enable direct comparison with model predictions. A validated model would allow safe, cost-effective evaluation of interventions without requiring further fall experiments.

Discussion on the statistical analysis

We evaluated models with different combinations of variables and used Bayesian Model Averaging to select the 'best' model. The problem of model selection has received substantial attention in the statistics literature. There are many approaches to this and conclusions on a 'best' model do not necessarily agree among methods. In an early analysis of the data, model choice was based on expected log predictive density (elpd) (Vehtari et al., 2017), implemented in the `loo`-package (Vehtari et al., 2020). Here one can choose between leave-one-out or leave-group-out cross-validation to estimate the elpd. The grouping by participant makes the second option a natural choice but is computationally very intensive. While it is feasible to compare a given set of models, to the best of the author's knowledge the `loo`-package does not provide a methodology to effectively screen through a large set of models. The BAS-package does allow for this, though it appears not easy to include the multilevel structure into it. For that reason, we have used the median probability model for variable selection and subsequently fitted the multilevel model described with (3). The resulting multilevel model turned out to give better LOO values than an initial search in the model space based on expert knowledge.

Experimental measurements of the MAHD

We determined the MAHD using a Bayesian multilevel logistic regression model. For participants in this study, mean MAHD values ranged from approximately 8 to 16 N ms across forward speeds of 6 to 18 km/h, with a standard deviation of 4 N ms. These results provide an initial estimate of the maximum handlebar disturbance cyclists can withstand. We recommend eliminating disturbances exceeding these values from the road environment, though direct comparison to real-world disturbances is currently limited by the lack of systematic data on their force and torque profiles.

Key cyclist characteristics predictive of fall outcome

We identified two key cyclist characteristics influencing MAHD: forward speed v and balance skill S.

Forward speed v was a strong predictor of MAHD (Fig. 8). Surprisingly, participants tolerated higher disturbances at lower speeds, contrary to expectations based on increased bicycle instability at low speeds (Meijaard et al., 2007). This likely reflects treadmill constraints: at higher speeds, cyclists approached the treadmill edge more rapidly, requiring faster responses.

Balance skill S also strongly predicted MAHD. We defined S pragmatically as the cyclist's ability to maintain a centred trajectory during undisturbed cycling. While skill to respond to disturbances may differ from undisturbed performance, our findings underscores the notion that our definition at least captures an important fraction of the cyclist's balancing skill.

Control effort E was not a significant predictor of MAHD, nor was it correlated with S (see the Supplementary Online Material). This aligns with findings from car-following studies, where task performance and effort show complex relationships (Abbink et al., 2011, 2012; Petermeijer et al., 2015). Cyclists, like drivers, may optimise performance to a level they consider sufficient rather than maximal.

Four other attributes — age, mass, length, and reaction time — showed limited predictive power (Fig. 8). The lack of an age effect was unexpected given older cyclists' overrepresentation in injury statistics (Weijermars et al., 2016; Boele-Vos et al., 2017; Boufous et al., 2012), but suggests that when faced with a disturbance, older cyclists can recover as well as younger ones in controlled conditions. The higher injury rate could also be attributed to elderly being more sensitive to injury than younger cyclists.

The absence of a mass effect likely reflects our focus on handlebar disturbances, which primarily influence lateral dynamics independent of the cyclist mass. Variations in centre of mass height were also small, potentially explaining the lack of a length effect.

Reaction time (τ) was also absent in the highest-ranked model, but this result is inconclusive. Approximately 150 observations showed implausibly low τ values due to noisy EMG signals. These were omitted, reducing dataset size and potentially biasing the result. Importantly, this measurement issue affected only the reaction time variable.

Finally, participant ID i emerged as an important predictor, suggesting that other unmeasured cyclist characteristics influence MAHD and require further investigation.

Other key variables influencing the MAHD prediction

In addition to cyclist characteristics, our study highlighted other important predictors of MAHD: bicycle state at disturbance onset and disturbance direction.

Although we aimed to apply disturbances during steady, upright cycling at the treadmill centre, small variations in lean angle and steer rate (±3° and ±1°/s, see online supplementary material) remained.

These small variations already significantly affected the MAHD. This observation aligns with expectations, as disturbances applied in the same direction as the cyclist was already steering at that time amplifies the effect.

Finally, the disturbance rotational direction also affected MAHD, potentially reflecting individual differences in dexterity, although this characteristic was not explicitly measured.

Practical implications

Our study aims to improve the practical use of bicycle dynamics and cyclist control models for proactively evaluating fall prevention interventions. This can provide valuable evidence on the effectiveness of a broader range of interventions, such as improved bicycle and infrastructure design and training programs. Such insights can support engineers, practitioners, and policymakers in selecting and promoting effective measures.

Beyond modelling, our experimental setup also has direct practical applications, such as screening individual fall risk or comparing bicycle designs. Further details are provided in the online supplementary material.

5. Conclusion

This study is the first to provide experimental data on cyclists falls under controlled disturbances. We conducted the controlled cyclist fall experiments with 24 participants and developed a Bayesian multilevel logistic regression model to predict the Maximum Allowable Handlebar Disturbance (MAHD), reflecting the maximum disturbance from which a cyclist can recover balance.

This dataset and model provide a valuable tool for validating bicycle dynamics and cyclist control models in fall scenarios and predicting MAHD thresholds.

We identified forward speed v and skill performance S — the ability to maintain balance and follow a centreline — as key predictors of the MAHD. Notably, age did not emerge as a significant factor. Incorporating v and S into cyclist control models can improve their practical application.

Our findings represent a step forward in applying bicycle dynamics and cyclist control models to proactively evaluate fall prevention interventions such as safer infrastructure or bicycle designs, and training programs.

CRediT authorship contribution statement

Marco M. Reijne: Writing – review & editing, Writing – original draft, Visualization, Validation, Software, Project administration, Methodology, Investigation, Formal analysis, Data curation, Conceptualization. **Frank H. van der Meulen:** Writing – review & editing, Supervision, Methodology, Funding acquisition, Conceptualization. **Arend L. Schwab:** Writing – review & editing, Visualization, Supervision, Methodology, Investigation, Conceptualization.

Declaration of generative AI use in writing

During the preparation of this work, the authors used OpenAI's ChatGPT in order to improve the readability and language of the text. After using this tool, the authors reviewed and edited the content as needed and take full responsibility for the content of the publication.

Funding

This study is part of the 'Citius Altius Sanius' project (P16-28 CAS) and funded by the Netherlands Organisation for Scientific Research (NWO).

Declaration of competing interest

The authors report no competing interests.

Acknowledgements

The authors express their gratitude to the participants of the experiment for their time and valuable contributions to this research. Special thanks to Jan van Frankenhuyzen for his assistance in designing and building the experimental setup. The authors also wish to thank Zasha van Hijfte and Judith Cueto Fernandez for their support and help during the experiments. Shannon van de Velde is acknowledged for developing and adapting the Bump'em system for the bicycle fall experiments, as well as for her support in conducting the experiments. The authors extend their thanks to Heike Vallery for providing access to the lab and the Rysen system. Royal Dutch Gazelle is gratefully acknowledged for providing two bicycles, and the authors appreciate the support of Maxon group and Speedgoat GmbH in correctly setting-up the software and necessary components for the experiments. The authors extend their thanks to the anonymous reviewers for their constructive feedback, which helped improve the clarity and quality of this manuscript.

Appendix A. Supplementary Online Material (SOM)

The Supplementary Online Material is hosted at: https://github.com/fmeulen/CyclingFall

Data availability

The data are available in an online Github repository. The link is stated in the manuscript.

References

Abbink, D.A., Mulder, M., Boer, E.R., 2012. Haptic shared control: Smoothly shifting control authority? Cogn. Technol. Work. 14, 19–28. http://dx.doi.org/10.1007/s10111-011-0192-5.

Abbink, D.A., Mulder, M., van der Helm, F.C.T., Mulder, M., Boer, E.R., 2011. Measuring neuromuscular control dynamics during car following with continuous haptic feedback. IEEE Trans. Syst. Man Cybern. B 41 (5), 1239–1249. http://dx.doi.org/10.1109/TSMCB.2011.2120606.

Alizadehsaravi, L., Moore, J.K., 2023. Bicycle balance assist system reduces roll and steering motion for young and older bicyclists during real-life safety challenges. PeerJ 11, e16206. http://dx.doi.org/10.7717/peerj.16206.

Andersérs, C., Andersson, J., Warner, H.W., 2024. The importance of individual characteristics on bicycle performance during alcohol intoxication. Traffic Saf. Res. 6, http://dx.doi.org/10.55329/vmgb9648, e000042–e000042.

Andersson, J., Patten, C., Wallén Warner, H., Andersérs, C., Ahlström, C., Ceci, R., Jakobsson, L., 2023. Bicycling during alcohol intoxication. Traffic Saf. Res. 4, http://dx.doi.org/10.55329/prpa1909.

Baker, C., Yu, X., Lovell, B., Tan, R., Patel, S., Ghajari, M., 2024. How well do popular bicycle helmets protect from different types of head injury? Ann. Biomed. Eng. 52 (12), 3326–3364. http://dx.doi.org/10.1007/s10439-024-03589-8.

Barbieri, M.M., Berger, J.O., 2004. Optimal predictive model selection. Ann. Statist. 32 (3), 870–897. http://dx.doi.org/10.1214/009053604000000238.

Bates, D., Mächler, M., Bolker, B., Walker, S., 2015. Fitting linear mixed-effects models using lme4. J. Stat. Softw. 67 (1), 1–48. http://dx.doi.org/10.18637/jss.v067.i01.

Beck, B., Stevenson, M., Newstead, S., Cameron, P., Judson, R., Edwards, E.R., Bucknill, A., Johnson, M., Gabbe, B., 2016. Bicycling crash characteristics: An in-depth crash investigation study. Accid. Anal. Prev. 96, 219–227. http://dx.doi.org/10.1016/j.aap.2016.08.012.

Boele-Vos, M.J., van Duijvenvoorde, K., Doumen, M.J.A., Duivenvoorden, C.W.A.E., Louwerse, W.J.R., Davidse, R.J., 2017. Crashes involving cyclists aged 50 and over in the Netherlands: An in-depth study. Accid. Anal. Prev. 105, 4–10. http://dx.doi.org/10.1016/j.aap.2016.07.016.

Boufous, S., de Rome, L., Senserrick, T., Ivers, R., 2012. Risk factors for severe injury in cyclists involved in traffic crashes in Victoria, Australia. Accid. Anal. Prev. 49, 404–409. http://dx.doi.org/10.1016/j.aap.2012.03.011.

Bruijn, S.M., Meijer, O.G., Beek, P.J., van Dieen, J.H., 2013. Assessing the stability of human locomotion: A review of current measures. J. R. Soc. 10 (83), 20120999. http://dx.doi.org/10.1098/rsif.2012.0999.

Bulsink, V.E., Kiewiet, H., van de Belt, D., Bonnema, G.M., Koopman, B., 2016. Cycling strategies of young and older cyclists. Hum. Mov. Sci. 46, 184–195. http://dx.doi.org/10.1016/j.humov.2016.01.005.

Bürkner, P.-C., 2017. Brms: An r package for Bayesian multilevel models using stan. J. Stat. Softw. 80, 1–28. http://dx.doi.org/10.18637/jss.v080.i01.

Clyde, M., 2022. BAS: Bayesian variable selection and model averaging using Bayesian adaptive sampling. R package version 1.6.4.
Clyde, M.A., Ghosh, J., Littman, M.L., 2011. Bayesian adaptive sampling for variable selection and model averaging. J. Comput. Graph. Statist. 20 (1), 80–101. http://dx.doi.org/10.1198/jcgs.2010.09049.
Crenshaw, J.R., Bernhardt, K.A., Atkinson, E.J., Khosla, S., Kaufman, K.R., Amin, S., 2018. The relationships between compensatory stepping thresholds and measures of gait, standing postural control, strength, and balance confidence in older women. Gait Posture 65, 74–80. http://dx.doi.org/10.1016/j.gaitpost.2018.06.117.
de Waard, D., Schepers, P., Ormel, W., Brookhuis, K., 2010. Mobile phone use while cycling: Incidence and effects on behaviour and safety. Ergonomics 53 (1), 30–42. http://dx.doi.org/10.1080/00140130903381180.
Dialynas, G., Christoforidis, C., Happee, R., Schwab, A.L., 2023. Rider control identification in cycling taking into account steering torque feedback and sensory delays. Veh. Syst. Dyn. 61 (1), 200–224. http://dx.doi.org/10.1080/00423114.2022.2048865.
Doll, R.J., Buitenweg, J.R., Meijer, H.G.E., Veltink, P.H., 2014. Tracking of nociceptive thresholds using adaptive psychophysical methods. Behav. Res. Methods 46 (1), 55–66. http://dx.doi.org/10.3758/s13428-013-0368-4.
Dubbeldam, R., Baten, C.T.M., Straathof, P.T.C., Buurke, J.H., Rietman, J.S., 2017. The different ways to get on and off a bicycle for young and old. Saf. Sci. 92, 318–329. http://dx.doi.org/10.1016/j.ssci.2016.01.010.
Elvik, R., 2001. Area-wide urban traffic calming schemes: A meta-analysis of safety effects. Accid. Anal. Prev. 33 (3), 327–336. http://dx.doi.org/10.1016/S0001-4575(00)00046-4.
Fahlstedt, M., Halldin, P., Kleiven, S., 2016. The protective effect of a helmet in three bicycle accidents — A finite element study. Accid. Anal. Prev. 91, 135–143. http://dx.doi.org/10.1016/j.aap.2016.02.025.
Gelman, A., Carlin, J., Stern, H., Dunson, D., Vehtari, A., Rubin, D., 2013. Bayesian Data Analysis, third ed. In: Chapman & Hall/CRC Texts in Statistical Science, Taylor & Francis, https://books.google.nl/books?id=ZXL6AQAAQBAJ.
Hellman, I.I., Lindman, M., 2023. Estimating the crash reducing effect of advanced driver assistance systems (ADAS) for vulnerable road users. Traffic Saf. Res. 4, http://dx.doi.org/10.55329/blzz2682, 000036–000036.
Hoeting, J.A., Madigan, D., Raftery, A.E., Volinsky, C.T., 1999. Bayesian model averaging: A tutorial (with comments by M. Clyde, David Draper and E. I. George, and a rejoinder by the authors). Statist. Sci. 14 (4), 382–417. http://dx.doi.org/10.1214/ss/1009212519.
Hoye, A., 2018. Recommend or mandate? A systematic review and meta-analysis of the effects of mandatory bicycle helmet legislation. Accid. Anal. Prev. 120, 239–249. http://dx.doi.org/10.1016/j.aap.2018.08.001.
Janssen, B., Schepers, P., Farah, H., Hagenzieker, M., 2018. Behaviour of cyclists and pedestrians near right angled, sloped and levelled kerb types: Do risks associated to height differences of kerbs weigh up against other factors? Eur. J. Transp. Infrastruct. Res. 18 (4), 360–371. http://dx.doi.org/10.18757/ejtir.2018.18.4.3254.
Keppner, V., Krumpoch, S., Kob, R., Rappl, A., Sieber, C.C., Freiberger, E., Siebentritt, H.M., 2023. Safer cycling in older age (SiFAr): Effects of a multi-component cycle training. a randomized controlled trial. BMC Geriatr. 23 (1), 131. http://dx.doi.org/10.1186/s12877-021-02502-5.
Kircher, K., Niska, A., 2024. Interventions to reduce the speed of cyclists in work zones — cyclists' evaluation in a controlled environment. Traffic Saf. Res. 6, http://dx.doi.org/10.55329/ohhx5659, e000047–e000047.
Kooijman, J.D.G., Meijaard, J.P., Papadopoulos, J.M., Ruina, A., Schwab, A.L., 2011. A bicycle can be self-stable without gyroscopic or caster effects. Science 332 (6027), 339–342. http://dx.doi.org/10.1126/science.1201959.
Lambert, B., 2018. A Student's Guide to Bayesian Statistics. Sage.
Lubbe, N., Wu, Y., Jeppsson, H., 2022. Safe speeds: Fatality and injury risks of pedestrians, cyclists, motorcyclists, and car drivers impacting the front of another passenger car as a function of closing speed and age. Traffic Saf. Res. 2, http://dx.doi.org/10.55329/vfma7555, 000006–000006.
Meijaard, J.P., Papadopoulos, J.M., Ruina, A., Schwab, A.L., 2007. Linearized dynamics equations for the balance and steer of a bicycle: A benchmark and review. Proc. R. Soc. A: Math. Phys. Eng. Sci. 463 (2084), 1955–1982. http://dx.doi.org/10.1098/rspa.2007.1857.
Moore, J.K., 2012. Human Control of a Bicycle (Ph.D. thesis). University of California, Davis, USA, https://www.researchgate.net/profile/Jason-Moore-23/publication/232200635_Human_Control_of_a_Bicycle/links/0fcfd5078c76753288000000/Human-Control-of-a-Bicycle.pdf.
Niska, A., Wenäll, J., 2019. Simulated single-bicycle crashes in the VTI crash safety laboratory. Traffic Inj. Prev. 20 (sup3), 68–73. http://dx.doi.org/10.1080/15389588.2019.1685090.
Niska, A., Wenäll, J., Karlström, J., 2022. Crash tests to evaluate the design of temporary traffic control devices for increased safety of cyclists at road works. Accid. Anal. Prev. 166, 106529. http://dx.doi.org/10.1016/j.aap.2021.106529.
Peng, Y., Chen, Y., Yang, J., Otte, D., Willinger, R., 2012. A study of pedestrian and bicyclist exposure to head injury in passenger car collisions based on accident data and simulations. Saf. Sci. 50 (9), 1749–1759. http://dx.doi.org/10.1016/j.ssci.2012.03.005.
Petermeijer, S.M., Abbink, D.A., Mulder, M., de Winter, J.C.F., 2015. The effect of haptic support systems on driver performance: A literature survey. IEEE Trans. Haptics 8 (4), 467–479. http://dx.doi.org/10.1109/TOH.2015.2437871.
Pijnappels, M., Reeves, N.D., Maganaris, C.N., van Dieen, J.H., 2008. Tripping without falling; lower limb strength, a limitation for balance recovery and a target for training in the elderly. J. Electromyography Kinesiol. 18 (2), 188–196. http://dx.doi.org/10.1016/j.jelekin.2007.06.004.
Plooij, M., Keller, U., Sterke, B., Komi, S., Vallery, H., Von Zitzewitz, J., 2018. Design of RYSEN: An intrinsically safe and low-power three-dimensional overground body weight support. IEEE Robot. Autom. Lett. 3 (3), 2253–2260. http://dx.doi.org/10.1109/LRA.2018.2812913.
Sayed, T., Zaki, M.H., Autey, J., 2013. Automated safety diagnosis of vehicle-bicycle interactions using computer vision analysis. Saf. Sci. 59, 163–172. http://dx.doi.org/10.1016/j.ssci.2013.05.009.
Schepers, P., Agerholm, N., Amoros, E., Benington, R., Bjørnskau, T., Dhondt, S., de Geus, B., Hagemeister, C., Loo, B.P.Y., Niska, A., 2015. An international review of the frequency of single-bicycle crashes (SBCs) and their relation to bicycle modal share. Inj. Prev. 21 (e1), e138–e143. http://dx.doi.org/10.1136/injuryprev-2013-040964.
Schepers, P., Stipdonk, H., Methorst, R., Olivier, J., 2017. Bicycle fatalities: Trends in crashes with and without motor vehicles in the Netherlands. Transp. Res. F: Traffic Psychol. Behav. 46, 491–499. http://dx.doi.org/10.1016/j.trf.2016.05.007.
Schmidt, C.M., Dabiri, A., Schulte, F., Happee, R., Moore, J.K., 2023. Essential bicycle dynamics for microscopic traffic simulation: An example using the social force model. In: The Evolving Scholar-BMD 2023, fifth ed. http://dx.doi.org/10.59490/649d4037c2c818c6824899bd.
Schwab, A.L., de Lange, P.D.L., Happee, R., Moore, J.K., 2013. Rider control identification in bicycling using lateral force perturbation tests. Proc. Inst. Mech. Eng. K: J. Multi- Body Dyn. 227 (4), 390–406. http://dx.doi.org/10.1177/1464419313492317.
Schwab, A.L., Meijaard, J.P., 2013. A review on bicycle dynamics and rider control. Veh. Syst. Dyn. 51 (7), 1059–1090. http://dx.doi.org/10.1080/00423114.2013.793365.
Schwab, A.L., Meijaard, J.P., Kooijman, J.D.G., 2012. Lateral dynamics of a bicycle with a passive rider model: Stability and controllability. Veh. Syst. Dyn. 50 (8), 1209–1224. http://dx.doi.org/10.1080/00423114.2011.610898.
Tan, G.R., Raitor, M., Collins, S.H., 2020. Bump'em: An open-source, bump-emulation system for studying human balance and gait. In: 2020 IEEE International Conference on Robotics and Automation (ICRA). Paris, France, http://dx.doi.org/10.1109/ICRA40945.2020.9197105, 1 June - 31 August 2020.
Twaddle, H., Schendzielorz, T., Fakler, O., 2014. Bicycles in urban areas: Review of existing methods for modeling behavior. Transp. Res. Rec. 2434 (1), 140–146. http://dx.doi.org/10.3141/2434-17.
Utriainen, R., O'Hern, S., Pöllänen, M., 2023. Review on single-bicycle crashes in the recent scientific literature. Transp. Rev. 43 (2), 159–177. http://dx.doi.org/10.1080/01441647.2022.2055674.
van der Horst, A.R.A., de Goede, M., de Hair-Buijssen, S., Methorst, R., 2014. Traffic conflicts on bicycle paths: A systematic observation of behaviour from video. Accid. Anal. Prev. 62, 358–368. http://dx.doi.org/10.1016/j.aap.2013.04.005.
Vehtari, A., Gabry, J., Magnusson, M., Yao, Y., Bürkner, P.-C., Paananen, T., Gelman, A., 2020. Loo: Efficient leave-one-out cross-validation and WAIC for Bayesian models. https://mc-stan.org/loo/.
Vehtari, A., Gelman, A., Gabry, J., 2017. Practical Bayesian model evaluation using leave-one-out cross-validation and WAIC. Stat. Comput. 27 (5), 1413–1432. http://dx.doi.org/10.1007/s11222-016-9696-4.
Vlakveld, W.P., Twisk, D., Christoph, M., Boele, M., Sikkema, R., Remy, R., Schwab, A.L., 2015. Speed choice and mental workload of elderly cyclists on e-bikes in simple and complex traffic situations: A field experiment. Accid. Anal. Prev. 74, 97–106. http://dx.doi.org/10.1016/j.aap.2014.10.018.
Weijermars, W., Bos, N., Stipdonk, H.L., 2016. Serious road injuries in the Netherlands dissected. Traffic Inj. Prev. 17 (1), 73–79. http://dx.doi.org/10.1080/15389588.2015.1042577.
Westerhuis, F., Fuermaier, A.B.M., Brookhuis, K.A., de Waard, D., 2020. Cycling on the edge: The effects of edge lines, slanted kerbstones, shoulder, and edge strips on cycling behaviour of cyclists older than 50 years. Ergonomics 63 (6), 769–786. http://dx.doi.org/10.1080/00140139.2020.1755058.